The Astrophysical Journal, 707:761–767, 2009 December 10 doi:10.1088/0004-637X/707/1/761

LAGRANGIAN STATISTICS OF DARK HALOS IN A ΛCDM COSMOLOGY

Jounghun Lee[1], Oliver Hahn[2], and Cristiano Porciani[2,3]
[1] Department of Physics and Astronomy, FPRD, Seoul National University, Seoul 151-747, Republic of Korea; jounghun@astro.snu.ac.kr
[2] Institute for Astronomy, ETH Zurich, CH-8093 Zürich, Switzerland
[3] Argelander Institut für Astronomie, Auf dem Hügel 71, D-53121 Bonn, Germany
Received 2009 June 28; accepted 2009 October 27; published 2009 November 25

ABSTRACT

New statistical properties of dark matter halos in Lagrangian space are presented. Tracing back the dark matter particles constituting bound halos resolved in a series of *N*-body simulations, we measure quantitatively the correlations of the proto-halo's inertia tensors with the local tidal tensors and investigate how the correlation strength depends on the proto-halo's sphericity, local density, and filtering scale. It is shown that the majority of the proto-halos exhibit strong correlations between the two tensors provided that the tidal field is smoothed on the proto-halo's mass scale. The correlation strength is found to increase as the proto-halo's sphericity increases, as the proto-halo's mass increases, and as the local density becomes close to the critical value, δ_{ec}. It is also found that those peculiar proto-halos which exhibit exceptionally weak correlations between the two tensors tend to acquire higher specific angular momentum in Eulerian space, which is consistent with the linear tidal torque theory. In the light of our results, it is intriguing to speculate a hypothesis that the low surface brightness galaxies observed at present epoch correspond to the peculiar proto-halos with extreme low sphericity whose inertia tensors are weakly correlated with the local tidal tensors.

Key words: cosmology: theory – large-scale structure of universe

1. INTRODUCTION

Galaxies are biased tracers of the underlying dark matter distribution. It has been well known that the two-point correlation function of the observed galaxies follows a power law, different from that of the dark matter determined in *N*-body simulations (e.g., Maddox et al. 1990). To test theoretical predictions based on the dark matter against real observations of galaxies, it is required to determine a hidden connection between the galaxies and dark matter. The density peak formalism was the first attempt to provide such a connection, according to which the galaxies form in the high peaks (i.e., local maxima) of the initial smoothed density field (Davis et al. 1985; Bardeen et al. 1986; Kaiser 1986; Bond & Myers 1996). Fitting quite well into the cold dark matter (CDM) paradigm and explaining successfully some observed properties of the galaxies, this density peak formalism became the most prevalent model for biased galaxy formation. Given that gravity is mainly responsible for the formation and evolution of the galaxies, it was indeed reasonable, appropriate, and natural to regard the initial density peaks as good indicators of the sites of galaxy formation.

An uncomfortable truth, however, had to be faced when Katz et al. (1993) reported the unexpected results derived from *N*-body simulations that the dark matter particles of galactic halos are not well overlapped with those from the high peaks of the initial density field. They traced the trajectories of dark matter particles that comprise the initial density peaks and found that the particles from the initial peaks do not end up in real halos. Furthermore, it was also shown that the correlation function of high density peaks is different from that of galactic halos. These disturbing results forced them to conclude that the high peaks of the initial density field cannot be good indicators of the sites of galaxy formation. In the same spirit, Porciani et al. (2002b) have shown that only ∼40% of the proto-halos in a *N*-body simulation contain a density peak within their Lagrangian volume and that gravitational shear plays an important role in shaping the proto-halos.

To find a good indicator of the initial sites of galaxy formation, it is first necessary to understand the statistical properties that the majority of the protogalactic sites possess in Lagrangian space. Such a property was first found unwittingly by Lee & Pen (2000) while studying the origin of the galaxy angular momentum. According to the linear tidal torque theory (Doroshkevich 1970; White 1984), the angular momentum of a protogalaxy is generated at first order only when the local tidal shear tensor is not perfectly correlated with the inertia–momentum tensor of the protogalaxy. In previous works dealing with the linear tidal torque theory (e.g., Catelan & Theuns 1996), it was assumed that the two tensors are generally uncorrelated. Lee & Pen (2000) tested the validity of this assumption against the numerical data from *N*-body simulations. They calculated the correlations between the two tensors at proto-halo sites and found for the first time that the two tensors are in fact quite strongly correlated with each other in contrast to the general assumption. Their result, however, was based on rather low-resolution *N*-body simulations and thus failed to draw serious attentions.

Later, Porciani et al. (2002b) re-tested this assumption against high-resolution simulations, confirming and extending the preliminary results of Lee & Pen (2000). Noting that the existence of strong correlations between the two tensors is such a common phenomenon exhibited by most of the proto-halos they considered, Porciani et al. (2002b) have suggested that the boundaries of the proto-halos are determined by the push and pull of the external mass distribution. This is in some sense the opposite of the common wisdom where the key factor is assumed to be the self-gravity attraction.

In this paper, we want to further improve upon the previous work by Lee & Pen (2000) and Porciani et al. (2002b) by using a more detailed statistical treatment and simulations of better quality. Our goal here is to quantify the correlations between the two tensors as new Lagrangian statistics of dark halos and investigate how the correlation strengths depend on proto-halo's shapes and local environments. The outline of this paper is as follows. In Section 2, a brief description of *N*-body data is provided

and the statistical analysis of it is presented. In Section 3, new Lagrangian statistics of dark halos related to the correlations of the proto-halo's inertia tensors with the local tidal tensors is presented. In Section 4, an implication of our result on the low surface brightness galaxies (LSBGs) is explained. In Section 5, the results are discussed and a final conclusion is drawn. Throughout this paper, we assume a spatially flat ΛCDM cosmology.

2. DATA AND ANALYSIS

We use the samples of dark matter halos obtained from three different *N*-body simulations conducted by Hahn et al. (2007) in periodic boxes of linear size $L_1 = 45\,h^{-1}$ Mpc, $L_2 = 90\,h^{-1}$ Mpc, and $L_3 = 180\,h^{-1}$ Mpc. All three simulations assume a spatially flat ΛCDM cosmology with $\Omega_m = 0.25$, $\Omega_\Lambda = 0.75$, $\Omega_b = 0.045$, $\sigma_8 = 0.9$, $H_0 = 0.73$, and $n_s = 1$, each following the evolution of 512^3 particles to the present epoch from a given initial redshift z_i (L_1, L_2, and L_3 have $z_i = 79$, $z_i = 65$, and $z_i = 52$, respectively). Bound halos were resolved in each simulation by applying the standard friends-of-friends algorithm with linking-length parameter of $b = 0.2l$, where l denotes the mean inter-particle distance (Efstathiou et al. 1985). Among them, only those halos comprising more than 300 dark matter particles were selected to avoid possible numerical artifacts. A total of 50,839 halos are selected (13,390, 16,339, and 21,110 halos from the L_1, L_2, and L_3 simulations, respectively), which span a wide mass range of [10.2, 15.3] in units of $h^{-1}\,M_\odot$. A full description of the simulations and the process of the halo-identification is provided in Hahn et al. (2007).

Tracing back to the initial conditions, the trajectories of dark matter particles that constitute each selected halo, we locate the proto-halo sites in the Lagrangian space corresponding to the initial epoch z_i. Then, we determine the center of mass of each proto-halo site using the positions of its constituent particles. At each halo's center of mass, we measure the mean density contrast δ in the initial density field smoothed with a top-hat filter of scale radius R_s. Here, we consider four different filtering scales: $R_s = 0.5$, 1, 2, and $5\,h^{-1}$ Mpc. The initial peculiar potential field ϕ was derived from the density field by solving the Poisson equation (Hahn et al. 2007), and the tidal shear tensor $\mathbf{T} \equiv (T_{ij})$ was measured as the second derivative of ϕ at the center of mass of each proto-halo. Diagonalizing $\mathbf{T}$, we determine the three eigenvectors $\{\mathbf{t}_1, \mathbf{t}_2, \text{and } \mathbf{t}_3\}$ corresponding to the three eigenvalues $\{\lambda_1, \lambda_2, \text{and } \lambda_3\}$ in a decreasing order.

The inertia momentum tensor $\mathbf{I} \equiv (I_{ij})$ of each proto-halo site is also determined using the positions of the constituent particles in accordance with the formula given in Hahn et al. (2007):

$$I_{ij} \equiv m_\alpha \sum_\alpha \left(r_\alpha^2 \delta_{ij} - x_{\alpha,j} x_{\alpha,k}\right), \quad (1)$$

where m_α is the mass of αth particle, $\mathbf{x}_\alpha$is the position vector of the αth particle from the center of mass of the proto-halo site, and δ_{jk} is the Kronecker symbol. When the correlations with the tidal field smoothed on the scale R_s are calculated, we consider only those halos whose mass M is in the range of $0.9M_s < M < 1.1M_s$, where M_s is the top-hat mass enclosed by the radius R_s, given the fact that a given proto-halo with mass M would experience the strongest effect from the tidal field smoothed on the same mass scale $M = M_s$ (Lee & Pen 2000; see also the Appendix in Hahn et al. 2009). Table 1 lists the number (N_h) and mean mass ($\bar{M}$) of halos considered for the correlations with the tidal field smoothed on the four different filtering radii R_s.

Table 1
Filtering Radius (R_s), the Top-Hat Mass (M_s) Enclosed by R_s, the Number of Halos (N_h) with Mass in Range of $[0.9M_s, 1.1M_s]$

R_s (h^{-1} Mpc)	M_s ($h^{-1}\,M_\odot$)	N_h
0.5	3.6×10^{10}	1049
1	2.9×10^{11}	1472
2	2.3×10^{12}	1835
5	3.6×10^{13}	145

A similarity transformation is performed to reexpress $\mathbf{I}$ in the principal frame of $\mathbf{T}$. To quantify the degree of the correlations between the two tensors, we define a parameter β as

$$\beta \equiv 1 - \left(\frac{\varrho_{12}^2 + \varrho_{23}^2 + \varrho_{31}^2}{\varrho_{11}^2 + \varrho_{22}^2 + \varrho_{33}^2}\right)^{1/2}, \quad (2)$$

where $\{\varrho_{11}, \varrho_{22}, \text{and } \varrho_{33}\}$ and $\{\varrho_{12}, \varrho_{23}, \text{and } \varrho_{31}\}$ represent the three diagonal and off-diagonal elements of $\mathbf{I}$ in the principal frame of $\mathbf{T}$, respectively. If a proto-halo region has a perfectly spherical shape, then the eigenvectors of its inertia tensor are degenerate (i.e., any axis frame can be its eigenvector system) and all of the off-diagonal elements of $\mathbf{I}$ are always zero ($\varrho_{12} = \varrho_{23} = \varrho_{31} = 0$). Thus, for the case of a perfectly spherical proto-halo region, we always have $\beta = 1$. When a proto-halo region is not perfectly spherical but its inertia tensor $\mathbf{I}$ is perfectly correlated with the tidal shear tensor $\mathbf{T}$ measured at its center of mass, then $\mathbf{I}$ should be completely diagonal in the principal axis frame of $\mathbf{T}$. Thus, for the case of a perfect correlation between $\mathbf{I}$ and $\mathbf{T}$, we will also have $\beta = 1$. On the other hand, if the two tensors are uncorrelated, then $\mathbf{I}$ in the principal axis frame of $\mathbf{T}$ is not diagonal and the off-diagonal elements should be as large as the diagonal ones in magnitude unless the eigenvectors of $\mathbf{I}$ are degenerate. As the strength of the correlations between $\mathbf{I}$ and $\mathbf{T}$ decreases, the degree of the deviation of β from the value of unity will increase.

In the following section, we determine the probability distribution of β and investigate how the value of β depends on the proto-halo's shape, local density, and filtering radius.

3. CORRELATIONS BETWEEN INERTIA AND TIDAL TENSORS

Using the numerical data described in Section 2, we first determine the probability density distribution, $p(\beta)$. Figure 1 shows $p(\beta)$ for the four different cases of $R_s = 0.5$, 1, 2, and $5\,h^{-1}$ Mpc (top-left, top-right, bottom-left, and bottom-right panel, respectively). It is worth mentioning again here that when we calculate β based on the tidal field smoothed on the scale R_s, we consider only those proto-halos whose masses belong to the range $(0.9M_s, 1.1M_s)$ with $M_s \equiv (4\pi/3)\bar{\rho}R_s^3$, where $\bar{\rho}$ is the mean mass density of the universe. In each panel, the error bars represent the Poissonian noise. In all cases, the distribution $p(\beta)$ is strongly biased toward the high-β section, reaching a maximum at $\beta \geqslant 0.9$. It is now clear that at the proto-halo sites the tidal shear and inertia momentum tensors are strongly correlated with each other, regardless of the smoothing scale, which confirms quantitatively the previous works (Lee & Pen 2000; Porciani et al. 2002b). Note also that for the case of $R_s = 0.5\,h^{-1}$ Mpc, a small number of proto-halos exhibit exceptionally low values of $\beta \leqslant 0.5$, while for the cases of $R_s = 1,\ 2, \text{and } 5\,h^{-1}$ Mpc all proto-halos have $\beta \geqslant 0.5$.

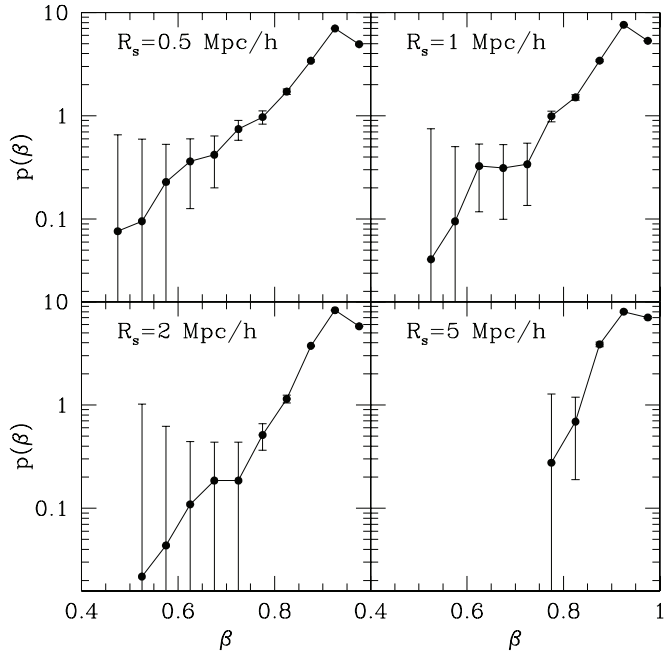

Figure 1. Probability density distribution of β of the protogalactic sites with Poissonian errors when the initial density field is smoothed on the scale of 0.5, 1, 2, and $5\,h^{-1}$ Mpc (top-left, top-right, bottom-left, and bottom-right, respectively).

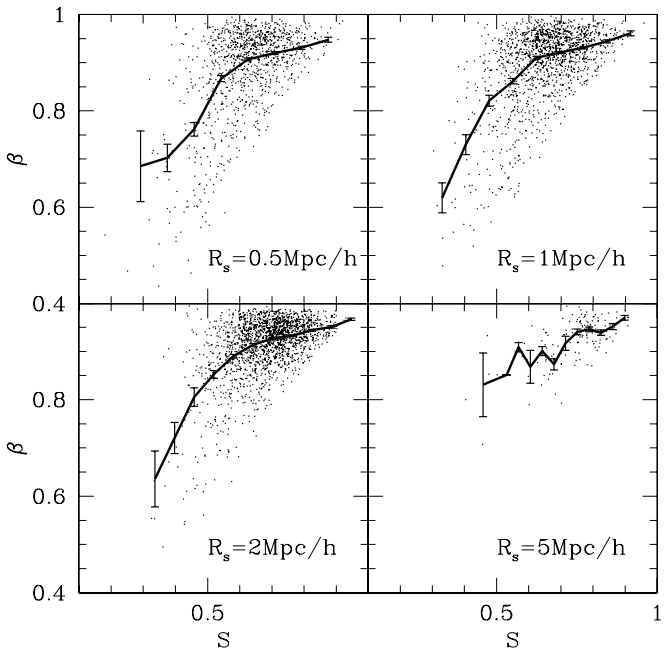

Figure 2. Scatter plots of β vs. the sphericity S of the proto-halo sites when the initial density field is smoothed on the scale of 0.5, 1, 2, and $5\,h^{-1}$ Mpc (top-left, top-right, bottom-left, and bottom-right, respectively). In each panel, the solid line represents the mean values $\langle\beta\rangle$ and the error bars indicate the standard deviation in the measurement of $\langle\beta\rangle$.

This result also implies that a halo of mass M tends to be made of those dark matter particles that accreted into the initial sites along the principal axes of the local tidal field smoothed on the same mass scale M, which is consistent with the Zel'dovich approximation (Zel'dovich 1970).

3.1. Dependence on Proto-halo's Sphericity and Linear Density

We investigate how β varies with the shapes of the proto-halos. Using the three eigenvalues of $\mathbf{I}$, we measure the sphericity S of each proto-halo as (Hahn et al. 2007)

$$S \equiv \left(\frac{\varrho_3}{\varrho_1}\right)^{1/2}, \tag{3}$$

where ϱ_1 and ϱ_3 represent the largest and the smallest eigenvalue of $\mathbf{I}$, respectively. Binning the range of S, we measure the mean of β averaged over a given differential bin, $[S, S + dS]$. Figure 2 shows the scatter plot of β versus S. The thick solid line corresponds to the mean value $\langle\beta\rangle$ as a function of S. The errors represent one standard deviation in the measurement of $\langle\beta\rangle$ calculated as $\langle\Delta\beta^2\rangle/\sqrt{(n-1)}$, where n represents the number of the proto-halos belonging to a given differential bin $[S, S+dS]$. It can be noted that β increases almost monotonically with S. In other words, the less spherical a proto-halo is, the weaker is the correlation between the tidal shear and the inertia momentum tensors. For those proto-halos with low sphericity ($S \leqslant 0.4$), the mean value, $\langle\beta\rangle$, drops below 0.7.

We also investigate how β changes with the local density field at the proto-halo sites. Let δ_i denote the initial density contrast measured at the proto-halo's center of mass. Since the three simulations used here started at different initial redshifts z_i (see Section 2), we use the linearly extrapolated linear density δ to $z = 0$ instead of δ_i itself, which is calculated as $\delta_L \equiv [D(z)/D(0)]\delta_i$, where $D(z)$ is the linear growth factor. We bin the range of δ and calculate the mean of β averaged

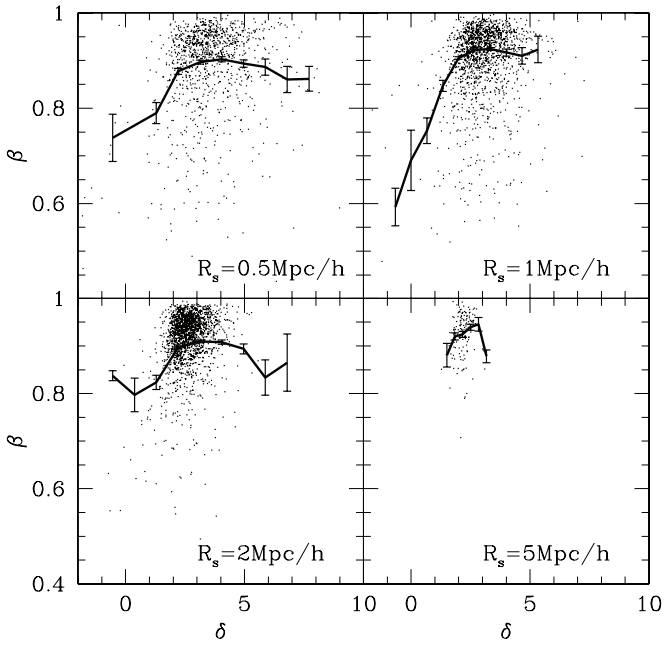

Figure 3. Scatter plots of β vs. the linearly extrapolated density δ of the proto-halo sites when the initial density field is smoothed on the scale of 0.5, 1, 2, and $5\,h^{-1}$ Mpc (top-left, top-right, bottom-left, and bottom-right, respectively). In each panel, the solid line represents the mean values $\langle\beta\rangle$ and the errors correspond to the one standard deviation in the measurement of $\langle\beta\rangle$.

over a given differential bin, $[\delta, \delta + d\delta]$. Figure 3 shows the scatter plots of β versus δ. The thick solid line corresponds to the mean value $\langle\beta\rangle$ as a function of δ. Note first that for the case of the large filtering radius $R_s = 5\,h^{-1}$ Mpc all values of δ lie in quite a narrow range converging to the critical density value $\delta_{ec} \approx 2.5$ for the ellipsoidal collapse (Sheth et al. 2001; Desjacques 2008; Robertson et al. 2009). In contrast, for the cases of smaller filtering radii $R_s = 0.5,\ 1$, and $2\,h^{-1}$ Mpc, the

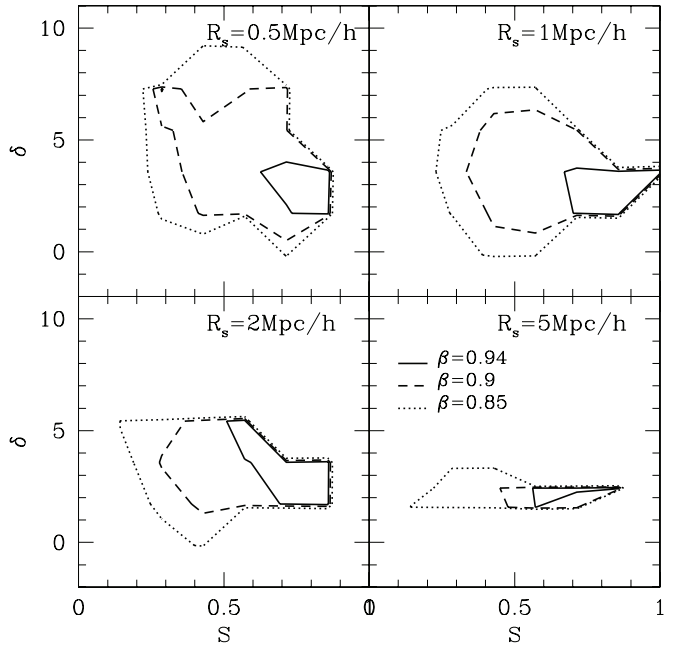

Figure 4. Contour plots of β in the S–δ when the initial density field is smoothed on the scale of 0.5, 1, 2, and $5\,h^{-1}$ Mpc (top-left, top-right, bottom-left, and bottom-right, respectively).

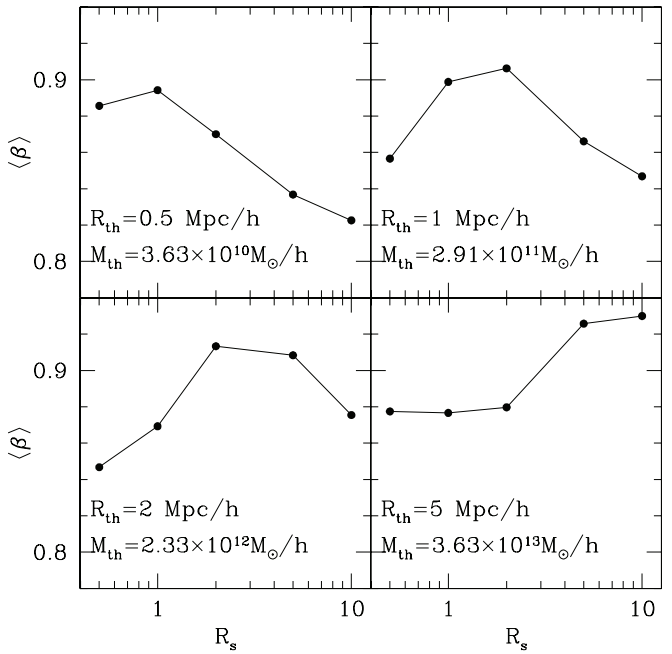

Figure 5. Mean values $\langle\beta\rangle$ as a function of the filtering radius R_s for four different values of the proto-halo masses. The four masses are enclosed by the four top-hat radii $R_{\rm th}$ as $M_{\rm th} = (4\pi/3)\bar{\rho}R_{\rm th}^3$, where $R_{\rm th} = 0.5,\ 1,\ 2$, and $5\,h^{-1}$ Mpc (top-left, top-right, bottom-left, and bottom-right, respectively).

values of δ spread over quite a wide range from -1 to 10. The value of β tends to be highest when δ becomes close to δ_{ec}. As δ deviates from δ_{ec}, the value of β decreases both in the high-δ and in the low-δ sections.

Since S and δ are not mutually independent but S tends to decrease in the low-δ region, it may be interesting to see how β varies as S and δ change simultaneously. Figure 4 shows the contour plots of β in the S–δ plane. This plot clearly demonstrates that those proto-halos with high S and $\delta \sim \delta_{ec}$ tend to have a high value of β.

3.2. Dependence on Filtering Scale

We now explore the dependence of β on the filtering radius. Let us consider two different scales $R_{\rm th}$ and R_s. We first calculate the inertia tensors of those halos whose masses lie in a fixed range of $(0.9M_{\rm th}, 1.1M_{\rm th})$, where $M_{\rm th}$ denotes the top-hat masses enclosed by the filtering scale $R_{\rm th}$. Then, we calculate the mean correlations $\langle\beta\rangle$ of these inertia tensors with the tidal tensors smoothed on the different scale of R_s. For each given $R_{\rm th}$, we consider four different scales R_s for the smoothing of the tidal tensors.

Figure 5 shows $\langle\beta\rangle$ as a function of the filtering scale R_s. Each panel plots the mean values of β calculated using the inertia tensors of the proto-halos with mass $M_{\rm th}$ enclosed by a fixed radius $R_{\rm th}$ and the tidal tensors smoothed on four different scales R_s. It can be seen that $\langle\beta\rangle$ increases monotonically when $R_s \leqslant 2R_{\rm th}$ and decreases sharply when $R_s > 2R_{\rm th}$. The value of β reaches a maximum when $R_{\rm th} \leqslant R_s \leqslant 2R_{\rm th}$. In terms of mass, it can be said that β becomes maximal at $M_{\rm th} \leqslant M_s \leqslant 8M_{\rm th}$. In other words, the inertia tensors of the proto-halos with masses $M_{\rm th}$ are strongly correlated with the local tidal fields smoothed on the mass scales that have the same order of magnitude as $M_{\rm th}$. If the tidal fields are smoothed on the scales of order of magnitude smaller or larger than $M_{\rm th}$, the correlations between the two tensors decrease. Thus, the correlation strength between the two tensors depends on the scale on which the tidal field is smoothed.

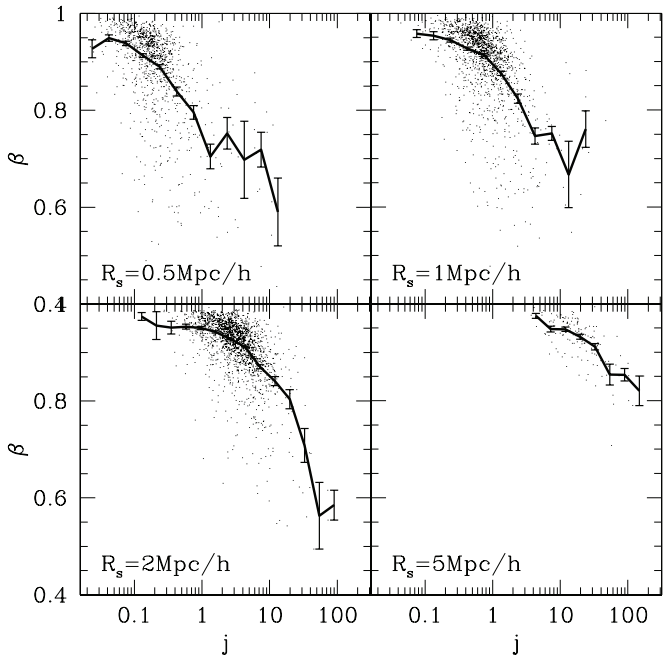

Figure 6. Scatter plots of β vs. the specific angular momentum j of the proto-halo sites when the initial density field is smoothed on the scale of 0.5, 1, 2, and $5\,h^{-1}$ Mpc (top-left, top-right, bottom-left, and bottom-right, respectively). In each panel, the solid line represents the mean values $\langle\beta\rangle(j)$ and the errors correspond to the one standard deviation in the measurement of $\langle\beta\rangle(j)$.

4. IMPLICATION ON THE LOW SURFACE BRIGHTNESS GALAXIES

In the light of our results, it is time to recall the linear tidal torque theory according to which the magnitude of the specific angular momentum (angular momentum per unit mass) of a proto-halo increases as the correlation of its inertia tensor with

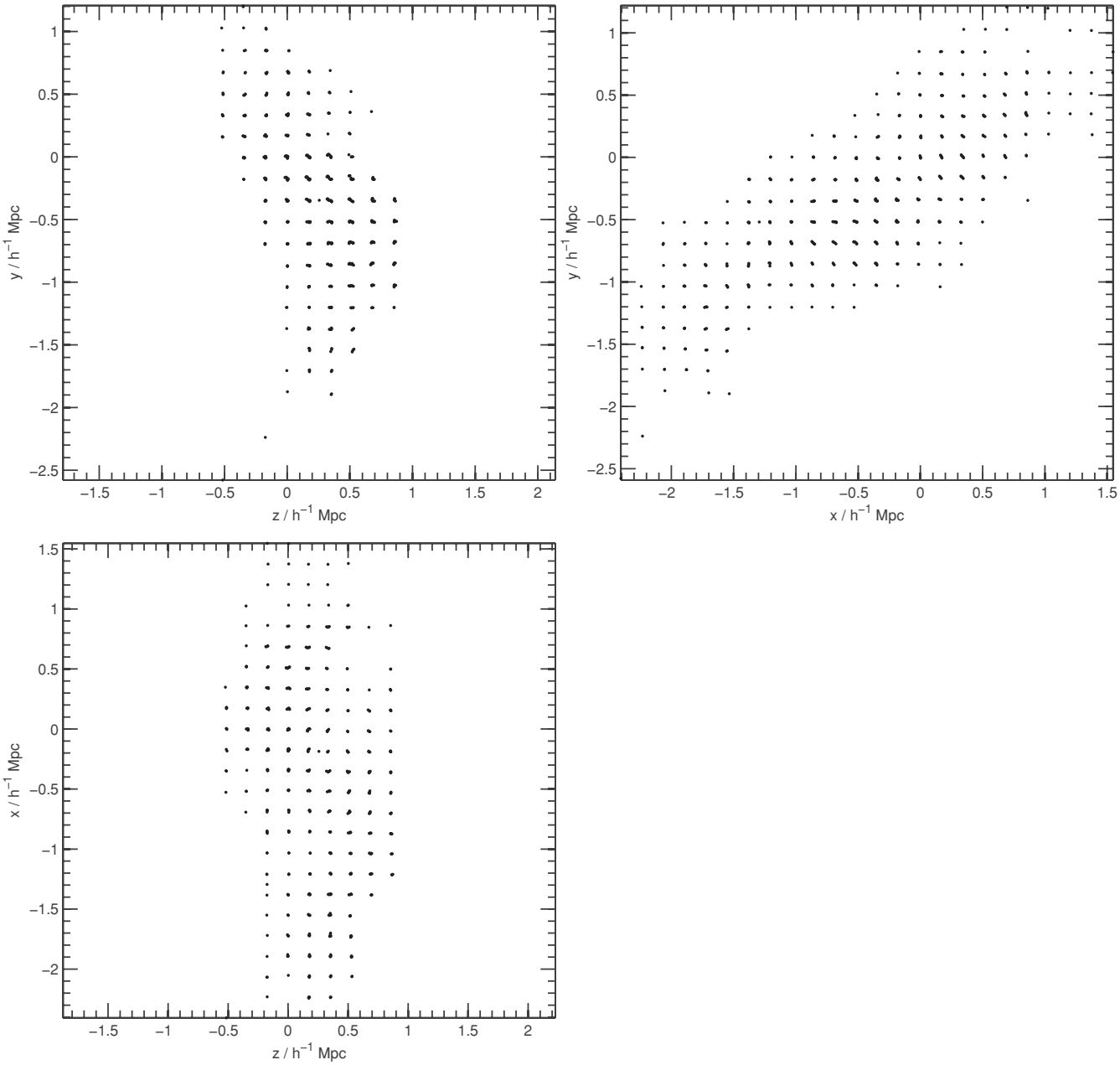

Figure 7. Particle distribution of a proto-halo with $S = 0.24$ in the x–y, y–z, and x–z plane in the top-left, top-right, and bottom-left panel, respectively.

the local tidal tensor increases (Doroshkevich 1970; White 1984; Catelan & Theuns 1996; Lee & Pen 2000). In the context of the linear tidal torque theory, those proto-halo sites which have low values of β are likely to acquire higher specific angular momentum (Porciani et al. 2002a). To test this core prediction of the linear tidal torque theory, we explore the dependence of β on the specific angular momentum measured in Eulerian space. For each halo, we first measure the angular momentum vector $\mathbf{J}$ in the Eulerian space as

$$\mathbf{J} \equiv \sum_{\alpha} m_{\alpha} \mathbf{r}_{\alpha} \times \mathbf{v}_{\alpha}, \tag{4}$$

where $\mathbf{r}_{\alpha}$ and $\mathbf{v}_{\alpha}$ represent the position and the velocity of the αth particle in the halo's center of mass frame, respectively. The specific angular momentum vector $\mathbf{j}$ of each halo is then calculated as $\mathbf{j} \equiv \mathbf{J}/M$. Binning the range of j, we calculate the mean of β averaged over a given differential bin, $[j, j + dj]$. Figure 6 shows the scatter plot of β versus j. The thick solid line corresponds to the mean value $\langle\beta\rangle(j)$ and the errors represent one standard deviation in the measurement of $\langle\beta\rangle(j)$. As can be seen, there is a strong trend that β increases with j. In other words, those proto-halos whose inertia tensors are less correlated with the local tidal tensors are likely to acquire higher specific angular momentum vectors in the subsequent evolution.

A crucial implication of our results is that the proto-halos with the lowest S will thus acquire the highest specific angular momentum since the proto-halos with the lowest S are found to have the weakest correlations between the inertia and tidal shear tensors (see Figure 2). It is very interesting to recall that the high-specific angular momentum is the characteristic property of the LSBGs (Boissier et al. 2003; Monnier Ragaigne et al. 2003, and references therein). Our result leads to a speculation that the LSBGs might originate from those peculiar proto-halos with

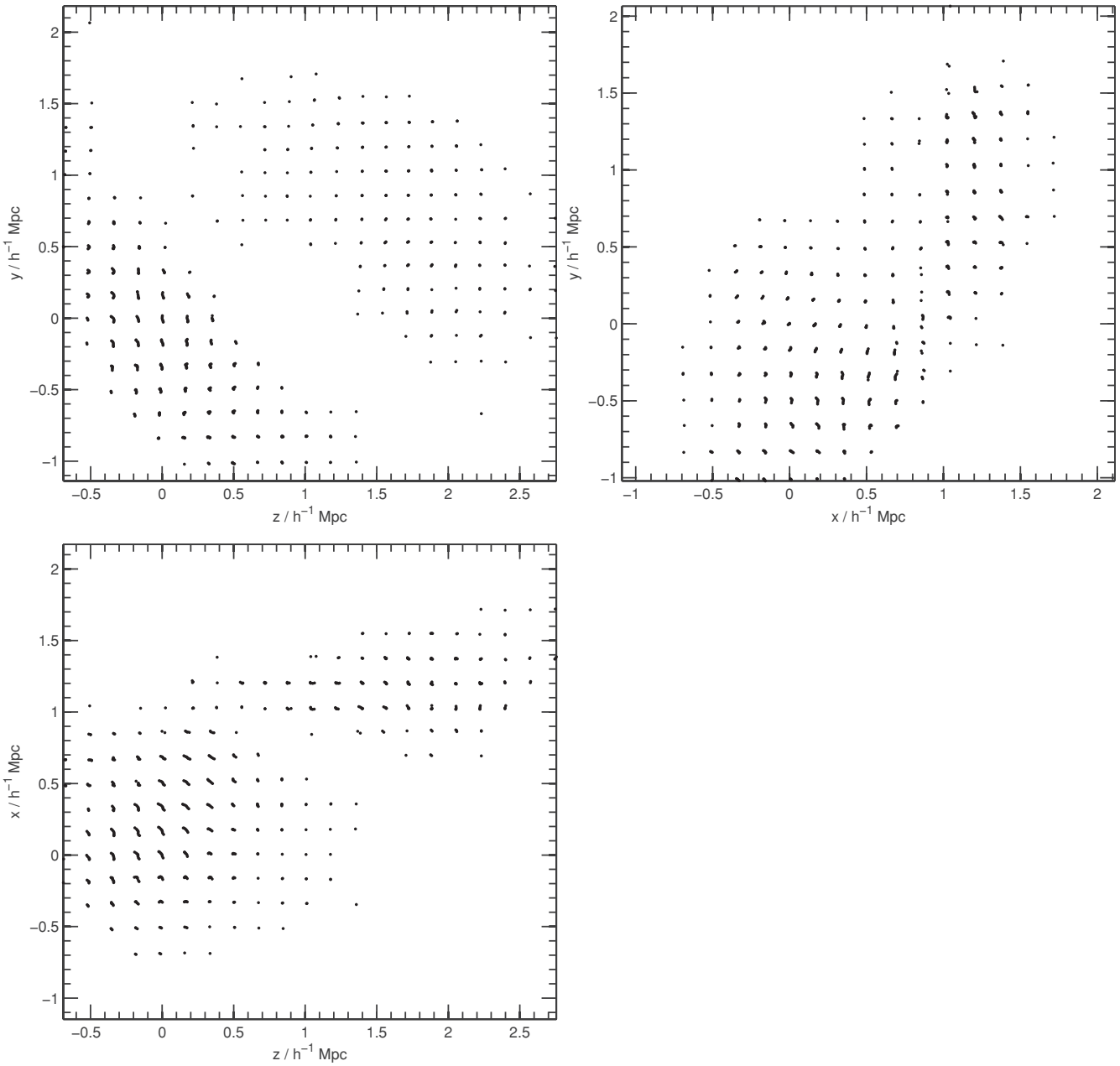

Figure 8. Same as Figure 7 but for the case of a disconnected proto-halo with $S = 0.25$.

very low values of S whose inertia tensors are weakly correlated with the local tidal tensors.

It is, however, worth mentioning here that the low values of S do not necessarily correspond to elongated particle distribution of proto-halo regions. A proto-halo region can have low values of S if it consists of two disconnected patches with center of mass located in the middle. To examine whether or not the proto-halos with low values of S have connected particle distribution, we inspect the particle distribution of those proto-halos with S below the tenth percentile in the mass range $2 \leqslant M/[10^{11}\, h^{-1}\, M_{\odot}] \leqslant 4$. We consider only the low-mass halos for this inspection since they exhibit the lowest values of S. It is found that among the inspected proto-halos, approximately two-thirds of them have connected particle distribution while the other one-third consist of more than two patches.

Figure 7 shows an example of a connected proto-halo, plotting its particle distribution in the z–y, x–y, and z–x plane in the top-left, top-right, and bottom-left panel, respectively. The sphericity of this example is as low as $S = 0.24$. As it can be seen, the Lagrangian region is connected, having indeed quite an elongated shape. Figure 8 shows an example of the disconnected proto-halo regions. Its sphericity is found to be $S = 0.25$. Strictly speaking, the first-order linear tidal torque theory is not valid to explain the generation of the angular momentum of such a disconnected proto-halo as shown in Figure 8. In this case, it might be the gravitational merging of the disconnected patches in the subsequent evolution rather than the misalignments between the inertia and tidal tensors in Lagrangian space that would contribute to the built-up of the higher angular momentum (Vitvitska et al. 2002).

Whether or not a proto-halo region is connected, however, the particles of a proto-halo region with lower value of β (and thus lower values of S) will end up in a final halo with higher specific angular momentum, as revealed in Figure 6. Therefore, it is

still possible to postulate that the peculiar proto-halos with low values of β correspond to the present LSBGs, no matter what caused the built-up of high angular momentum of the LSBGs.

5. DISCUSSION AND CONCLUSION

In the classical Zel'dovich model (Zel'dovich 1970), the inertia tensors of bound objects are perfectly correlated with the local tidal tensors in Lagrangian space. In practice, the two tensors are found to be indeed strongly but not perfectly correlated (Lee & Pen 2000; Porciani et al. 2002b). Here, we have determined quantitatively how the strengths of the correlations between the two tensors depend on proto-halo's shape and mass, local density, and filtering scale. Since the proto-halos form through the tidal flows of dark matter particles along the principal axes of the local tidal fields from the surrounding matter distribution, it is in fact natural to expect strong correlations between the two tensors. Deviations from the perfect correlations of the two tensors imply the existence of higher order perturbations from the simple tidal flows of CDM particles.

We have also found that for the peculiar proto-halos with low-S the correlations between the two tensors tend to be weak (i.e., having low value of β). Since those proto-halos which exhibit lower value of β end up in halos with higher specific angular momentum, it is intriguing to speculate a hypothesis that those peculiar proto-halos with lowest values of S would develop into the LSBGs at present epoch. Since the LSBGs are believed to be dark matter dominated, their density profiles are often directly compared with that of the dark halos (i.e., Navarro–Frenk–White (NFW) profile; Navarro et al. 1996), and the shallow inner-core slope of the observed density profiles of LSGBs has been used as a counterevidence for the CDM paradigm (e.g., Moore 1994). For instance, Kuzio de Naray et al. (2008) have recently studied the rotation curves of 17 LSBGs obtained from the high-resolution optical velocity fields from DensePak spectroscopic observations and shown that the observed LSBGs can be matched with the NFW halos only if the LSBGs have 20 km s^{-1} non-circular motions. If the LSBGs originate from the peculiar proto-halo sites with exceptionally low value of β as in our hypothesis, then their proto-halo sites may have had very low sphericity as our results imply. Those peculiar proto-halo sites which have extremely low sphericity at the initial stages might as well develop non-circular motions.

It will be interesting to study numerically the density profiles of those proto-halos with exceptionally low values of β and compare them with the standard NFW ones. It will be also interesting to compare the number density of those proto-halos with low values of β with that of the observed LSBGs as a function of mass. We plan to work on these two projects and hope to report the results elsewhere in the future.

We thank an anonymous referee for a very helpful report. J.L. acknowledges the financial support from the Korea Science and Engineering Foundation (KOSEF) grant funded by the Korean Government (MOST, no. R01-2007-000-10246-0). O.H. acknowledges support from the Swiss National Science Foundation. All simulations were performed on the Gonzales cluster at ETH Zurich, Switzerland.

REFERENCES

Bardeen, J. M., Bond, J. R., Kaiser, N., & Szalay, A. S. 1986, ApJ, 304, 15
Boissier, S., Monnier Ragaigne, D., Prantzos, N., van Driel, W., Balkowski, C., & O'Neil, K. 2003, MNRAS, 343, 653
Bond, J. R., & Myers, S. T. 1996, ApJS, 103, 1
Catelan, P., & Theuns, T. 1996, MNRAS, 282, 436
Davus, M., Efstathious, G., Frenk, C. S., & White, S. D. M. 1985, ApJ, 292, 371
Desjacques, V. 2008, MNRAS, 388, 638
Doroshkevich, A. G. 1970, Astrofizika, 6, 581
Efstathiou, G., Davis, M., White, S. D. M., & Frenk, C. S. 1985, ApJS, 57, 241
Hahn, O., Porciani, C., Carollo, C. M., & Dekel, A. 2007, MNRAS, 375, 489
Hahn, O., Porciani, C., Dekel, A., & Carollo, C. M. 2009, MNRAS, 398, 1742
Kaiser, N. 1986, Inner Space/Outer Space: The Interface between Cosmology and Particle Physics (Chicago, IL: Univ. Chicago Press), 258
Katz, N., Quinn, T., & Gelb, J. M. 1993, MNRAS, 265, 689
Kuzio de Naray, R., McGaugh, S. S., & de Blok, W. J. G. 2008, ApJ, 676, 920
Lee, J., & Pen, U.-L. 2000, ApJ, 532, L5
Maddox, S. J., Efstathiou, Sutherland, G. W. J., & Loveday, J. 1990, MNRAS, 242, 43P
Monnier Ragaigne, D., van Driel, W., Schneider, S. E., Jarrett, T. H., & Balkowski, C. 2003, A&A, 405, 99
Moore, B. 1994, Nature, 370, 629
Navarro, J. F., Frenk, C. S., & White, S. D. M. 1996, ApJ, 462, 563
Porciani, C., Dekel, A., & Hoffman, Y. 2002a, MNRAS, 332, 325
Porciani, C., Dekel, A., & Hoffman, Y. 2002b, MNRAS, 332, 339
Robertson, B. E., Kravtsov, A. V., Tinker, J., & Zentner, A. R. 2009, ApJ, 696, 636
Sheth, R. K., Mo, H. J., & Tormen, G. 2001, MNRAS, 323, 1
Vitvitska, M., Klypin, A. A., Kravtsov, A. V., Wechsler, R. H., Primack, J. R., & Bullock, J. S. 2002, ApJ, 581, 799
White, S. D. M. 1984, ApJ, 286, 38
Zel'dovich, Ya. B. 1970, A&A, 5, 84